# Central Serous Chorioretinopathy 18

Angie H.C. Fong and Timothy Y.Y. Lai

## Contents



A.H.C. Fong, FRCS • T.Y.Y. Lai, FRCS, FRCOphth (✉)
Department of Ophthalmology and Visual Sciences, The Chinese University of Hong Kong, Hong Kong, China
e-mail: tyylai@cuhk.edu.hk

## 18.1 Introduction

### 18.1.1 Definition and Pathogenesis

Central serous chorioretinopathy (CSC) was originally described by Albrecht von Graefe in



C.H. Meyer et al. (eds.), *Spectral Domain Optical Coherence Tomography in Macular Diseases*,
DOI 10.1007/978-81-322-3610-8_18

1866 as "central recurrent retinitis" (Von Graefe 1866). Since then our understanding of CSC has progressed considerably. Gass in 1967 named the disease as central serous chorioretinopathy and proposed choriocapillaris hyperpermeability as the cause of CSC (Gass 1967). This hypothesis was later supported by studies using indocyanine green angiography (ICGA) which showed multifocal areas of choroidal vascular hyperpermeability in eyes with CSC.

CSC is characterized by serous retinal detachment of the neurosensory retina at the posterior pole, sometimes associated with serous detachment of the retinal pigment epithelium (RPE). It is thought that the pathogenic mechanism for CSC is associated with a hyperdynamic choroidal circulation. The resulting elevated hydrostatic pressure of choroid causes elevation of the RPE, which in turn causes serous pigment epithelial detachments (PEDs). RPE might subsequently undergo tiny rips, which causes leakage into the subretinal space leading to neurosensory retinal detachment (Nicholson et al. 2013; Ross et al. 2011). Factors such as elevated serum glucocorticoid, *Helicobacter pylori* infection, and gene polymorphisms (eg, complement factor H) have been suggested to contribute to the pathogenesis of CSC (Miki et al. 2014).

### 18.1.2 Epidemiology

CSC develops more frequently in men, with a male to female ratio of approximately six to one. The mean age of onset is around 41 years of age, but CSC can be found in young patients or in patients over 60 years old. The disease occurs most frequently in Asians and Whites and less frequently in the African-American populations, although the disease appeared to behave more aggressively in blacks (Ross et al. 2011). CSC is usually unilateral at initial presentation; however, bilateral cases have been reported to occur in up to 40 %. Chronic cases of CSC tend to have bilateral involvement (Gäckle et al. 1998a, b).

### 18.1.3 Natural History

Traditionally, CSC was thought to be a benign and self-limiting condition (Gass 1967). However, we now classify CSC broadly into acute (or classic) and chronic forms. Only the acute form carries a favorable prognosis of being a self-limiting condition, in which the serous macular detachment usually resolves after 3 months. Although these cases with acute CSC are usually not associated with loss of visual acuity, subtle changes in retinal sensitivity and contrast may occur (Bajarboura 2001). The chronic cases can be divided into chronic CSC following a single episode, recurrent resolving CSC, and recurrent chronic CSC. The proportion of eyes with recurrent CSC has been estimated to be around 30 % (Castro-Correia et al. 1992). The chronic form of CSC is sometimes characterized by diffuse RPE change, indicating widespread decompensation of the RPE, and has been referred to as diffuse retinal pigment epitheliopathy (DRPE) (Polak et al. 1995). The chronic subretinal fluid could be absorbed by the RPE due to diffuse dysfunction and loss of RPE, and the presence of fluid causes progressive photoreceptor death and may result in permanent visual loss (Nicholson et al. 2013).

Another rare form of CSC is the bullous variant, characterized by inferiorly gravitating fluid causing bullous exudative retinal detachment. It can be primary or associated with the use of systemic corticosteroid, organ transplant, and pregnancy (Gass 1973). Favorable outcome has been described for these cases which tend to be self-limiting. Otsuka and colleagues described a series of 25 cases of bullous CSC in which 52 % achieved a visual acuity of 20/20 or better and 80 % achieved 20/40 (Otsuka et al. 2002).

### 18.1.4 Why Spectral-Domain Optical Coherence Tomography (SD-OCT) Is Useful in Central Serous Chorioretinopathy?

OCT is one of the primary imaging techniques used in the diagnosis and management of

CSC. Compared with time-domain OCT (TD-OCT), spectral-domain OCT (SD-OCT) has a 43–100 times higher image acquisition speed. It has a higher signal-to-noise ratio and can capture high-quality images of retinal microstructures up to 1 μm axial resolution (Wojtkowski et al. 2005). SD-OCT provides a convenient, noninvasive way to evaluate the presence and resolution of subretinal fluid and other pathology in CSC. Changes in the photoreceptor layers, outer nuclear layer (ONL), or the external limiting membrane (ELM) can be clearly visualized. Visualization of these structures is useful because the ELM, ONL thickness, and the continuity of the photoreceptor inner and outer segment (IS/OS) junction are positively correlated with visual function and carries important prognostic significance. Also, using eye-tracking device, the same cross-sectional area can be scanned at each visit, so that the morphological changes at the same location can be accurately evaluated longitudinally. Early macular changes in CSC such as shallow subretinal fluid or serous PED might be subtle and missed on fundus examination, but these changes will be clearly visualized in SD-OCT examination.

As the main pathology of CSC lies in the choroid, imaging of the choroid is important in the evaluation of CSC. Enhanced depth imaging OCT (EDI-OCT) is such an imaging technique that is now commercially available with various SD-OCT machines. In EDI-OCT, the choroid is placed closer to the zero-delay plane compared with the retina, thus placing the most focused portion of the OCT scan on the choroid. An enhanced image of the choroid, from the Bruch's membrane to the suprachoroidal space, can then be obtained. This is a useful tool to provide in vivo cross-sectional histological information of choroidal vessels, as well as choroidal thickness, in normal and disease states.

Another new development using the SD-OCT is the coronal imaging or en face OCT imaging. Using three-dimensional reconstruction of transverse images of SD-OCT, a virtual "macula block" can be imaged, and coronal sections recreated from these scans, otherwise known as the C-scan or en face OCT. Using this technology, coronal sections of the retina, subretinal space, and choroid can be visualized, allowing collection of new information that complements other investigations. For example, choroidal venous dilatation under the abnormal RPE can be visualized on en face EDI-OCT whereby it will only appear as a hyperdynamic circulation on ICGA.

## 18.2 SD-OCT Changes and Findings in Central Serous Chorioretinopathy

### 18.2.1 Subretinal Fluid in Central Serous Chorioretinopathy

The hallmark of CSC is the accumulation of subretinal fluid (SRF) under the neurosensory retina causing a serous retinal detachment (SRD) (Fig. 18.1). Three-dimensional analysis of the SRF configuration in CSC using SD-OCT shows that the morphology of SRF in CSC changes over time (Ahn et al. 2013). The height of the SRD is higher in acute CSC compared with chronic CSC (Song et al. 2012). Ahn and colleagues evaluated the ratio of peak height to the greatest basal diameter of the SRD and found that the ratio was higher in acute than chronic CSC (Ahn et al. 2013) (Fig. 18.1). Early dynamic changes in SRF are more often observed in acute than chronic CSC, and the changing pattern differs according to prognosis. Eyes with spontaneous resolution often show symmetrical shrinking of SRF, while eyes with persistent fluid showed flattening and elongation of the SRF, turning the basal area into an oval shape. It is possible that the inferior shifting of SRF as observed in OCT is a result of the gravitational effect on the SRF, which is greater with persistent SRF in chronic CSC. Fluorescein angiography (FA) has demonstrated inferior gravitational tracts often described as hourglass configuration which can be seen extending from the macula to the inferior retina in chronic CSC eyes, where the SRF dissects its way down through

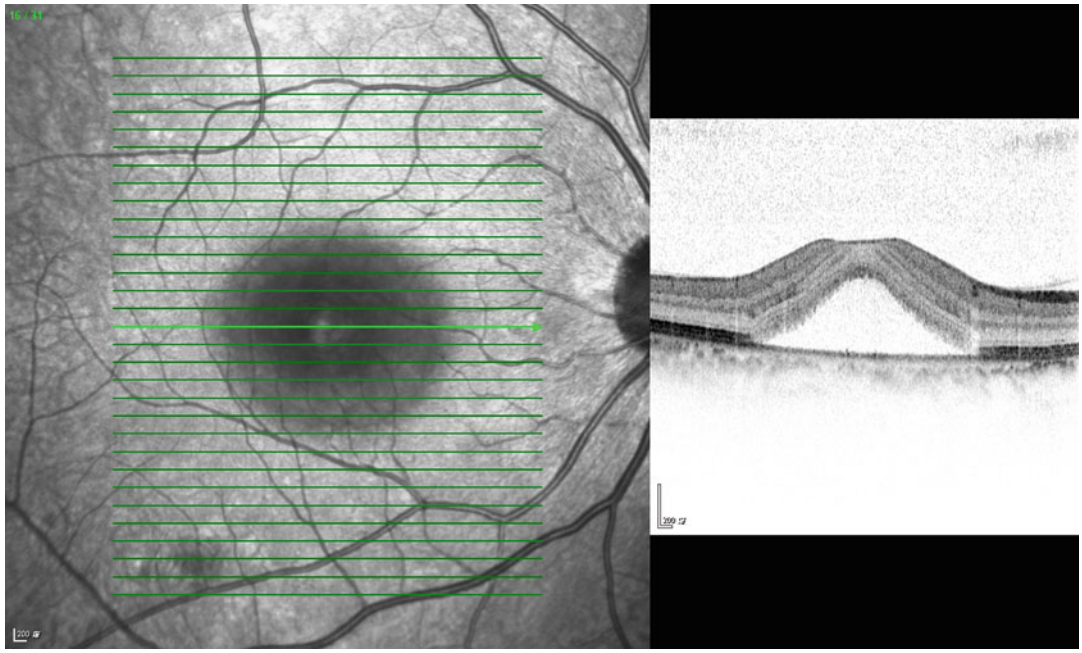

**Fig. 18.1** Acute central serous chorioretinopathy. SD-OCT showing high height of subretinal fluid relative to the basal diameter of the fluid

the subretinal space due to a high specific gravity (Yannuzzi et al. 1984).

### 18.2.2 Fibrin in Central Serous Chorioretinopathy

As early as 1967, Gass reported the presence of cloudy white exudate surrounding PED in patients with CSC with accompanying evidence of angiographic leakage (Gass 1967). Subsequent studies found that fibrin is present from 19 to 62 % of eyes with CSC (Ooto et al. 2010; Shinojima et al. 2010; Kim et al. 2012; Nair et al. 2012). The presence of fibrin indicates serous exudate, rich in protein, pigment granules, or homogeneous hyaline-like masses (Gass 1967). Fibrin appears as a hyper-reflective lump in the subretinal space on SD-OCT (Fig. 18.2), often overlying small PED, corresponding to leakage sites on FA (Kim et al. 2012). En face OCT scanning often shows a break in the PED associated with fibrin indicating active leakage from these PEDs. Shinjojima and colleagues visualized fibrin-like substance beneath the RPE in 62 % of eyes and suggested that plasma components, including fibrinogen, might be released from choriocapillaris and form fibrin beneath RPE, which leak into the subretinal space through defects in the RPE (Shinojima et al. 2010). Smooth protrusions of the RPE are also associated with fibrin in eyes with CSC.

In eyes with acute CSC, characteristic focal dipping or sagging of the posterior retina (Fujimoto et al. 2008; Song et al. 2012; Nair et al. 2012; Kim et al. 2012) could be seen accompanying fibrin over the leakage site in up to 38 % of eyes at a mean of 8 days after disease onset (Song et al. 2012) (Fig. 18.3). Song et al. suggested that this might be a result of a focal residual attachment of the retina with reactive exudation that persisted until the detachment of neurosensory retina from the RPE was complete. Therefore, focal dipping or sagging of the posterior retina associated with fibrin may be an early indicator of acute CSC. Subretinal fibrinous exudates were observed in around 24 % of eyes with early chronic CSC in their study that persisted into the late chronic stage.

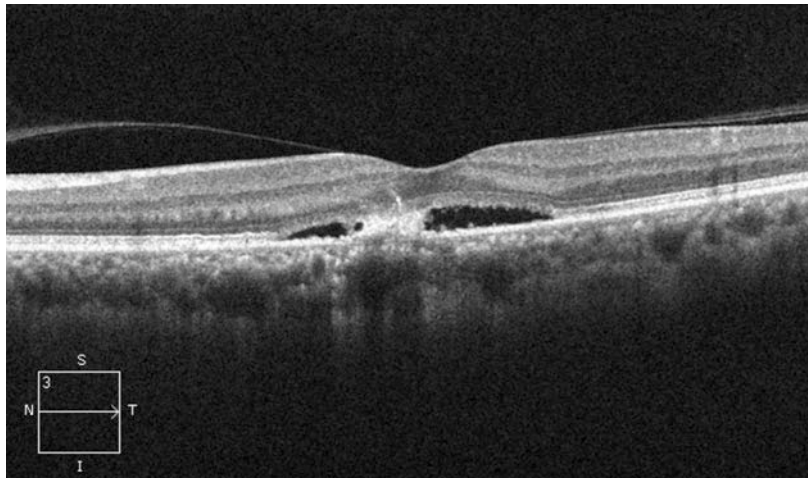


**Fig. 18.2** Fibrin in central serous chorioretinopathy. SD-OCT scan showing subretinal fluid with hyper-reflective material due to fibrin in acute central serous chorioretinopathy

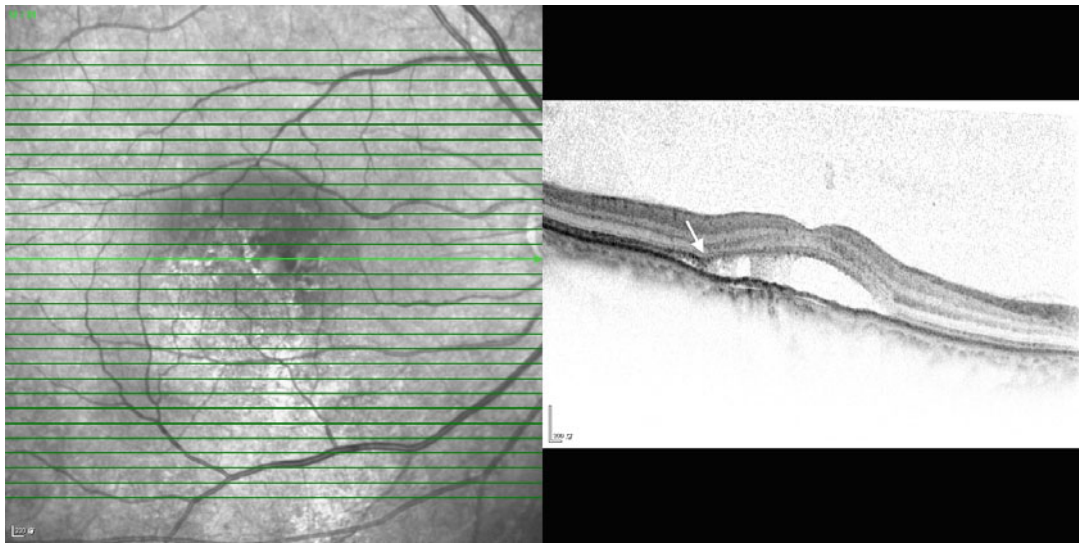

**Fig. 18.3** SD-OCT showing fibrin in the subretinal fluid with focal dipping (*arrow*) of the posterior retina in acute central serous chorioretinopathy

### 18.2.3 Central Serous Chorioretinopathy with Bullous Serous Retinal Detachment

Gass in 1973 first described a series of five cases of bullous exudative retinal detachment as an unusual manifestation of CSC (Gass 1973). This rare presentation is thought to be an exaggerated form of typical CSC. Clinically, there is bullous retinal detachment with shifting subretinal fluid. There are large, single, or multiple-leaking PEDs which are often hidden under cloudy subretinal exudation (Sahu et al. 2000). FA reveals multiple foci of intense RPE leakage communicating with the detached subretinal space (Fig. 18.4). It is thought that proteins and fibrinogen escape into the subretinal space through these intensive leakage sites leading to the presence of a thick subretinal exudate which subsequently seals the

leakage site (Fig. 18.5). Fibrin may also stimulate the fibrosis leading to formation of subretinal fibrotic membrane (Hooymans 1998; Schatz et al. 1995).

On SD-OCT scans, bullous neurosensory retinal detachments and large PEDs could be visualized. Spontaneous RPE rip appearing as a defect in the RPE with a rolled edge has also been reported (Lee et al. 2013) (Fig. 18.6). Due to the bullous appearance, bullous CSC might be mistaken with other diseases such as rhegmatogenous retinal detachment, idiopathic uveal effusion syndrome, multifocal choroiditis, Vogt-Koyanagi-Harada disease, choroidal metastasis, or lymphoma (Gass and Little 1995). Bullous CSC can be idiopathic in healthy individuals or can occur following high-dose corticosteroid therapy, organ transplantation, and hemodialysis or in pregnant women. Although most cases of bullous retinal detachment in CSC resolve either spontaneously, with discontinuation of steroid, following delivery or after laser photocoagulation, the visual outcome is usually variable. One series reported visual deterioration in all bullous CSC patients with 50 % having a final vision of 20/200 or worse, while others reported a good outcome with 80 to 100 % achieving vision of 20/40 or better (Fawzi et al. 2006; Gass 1973, 1991, 1992; Gass and Little 1995; Sahuet al. 2000).

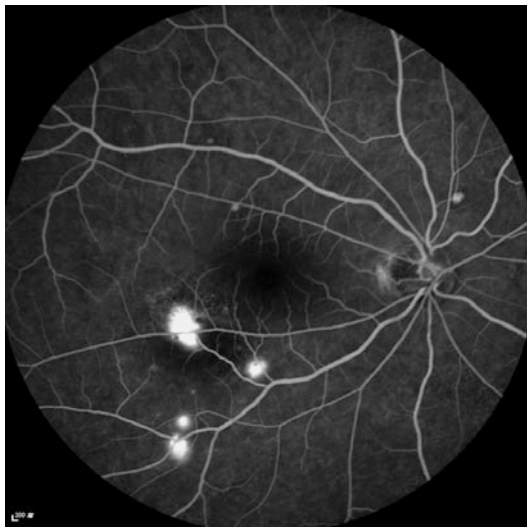

**Fig. 18.4** Bullous central serous chorioretinopathy. Mid-phase fluorescein angiography of an eye showing multiple leakage sites

### 18.2.4 Degeneration of Photoreceptors and Outer Retinal Changes in Central Serous Chorioretinopathy

The inner segment/outer segment (IS/OS) junction of the photoreceptors, also known as the ellipsoid zone (EZ), shows up as a hyperreflective line on OCT scans and has been found to be closely related to visual acuity. In normal individuals, the IS/OS line is continuous at the macula, while the IS/OS line is disrupted in various disease states. In CSC, the IS/OS line is usually not visible in eyes with serous retinal detachment but becomes visible again in the majority of eyes after resolution of the subretinal fluid (Kim et al. 2012). This indicates a disruption of the normal photoreceptor assembly during the serous macular detachment, which normalizes with phagocytosis of photoreceptor shed discs by the RPE upon reattachment.

During the acute phase of CSC, there is elongation of the photoreceptor OS, which is seen on SD-OCT as a thickened and smooth posterior surface of the detached retina (Ooto et al. 2011; Song et al. 2012). After several months, the posterior surface of the detached retina takes on a granulated or partially thinned appearance, and hyper-reflective dots begin to appear intraretinal or on the posterior retinal surface, reflecting accumulation of shed OS (Fujimoto et al. 2008; Kim et al. 2012; Ojima et al. 2007) (Fig. 18.7). In the late phase of CSC, the posterior surface of the retina is usually thinned due to long-standing shedding and disintegration of the photoreceptors. A chronic sustained serous retinal detachment results in the disruption of the outer photoreceptor layer, and atrophy of the RPE ensues.

SD-OCT findings of IS/OS line discontinuity, longer length of IS/OS disruption, thinning of the outer nuclear layer, disruption in external limiting membrane integrity, presence of hyper-

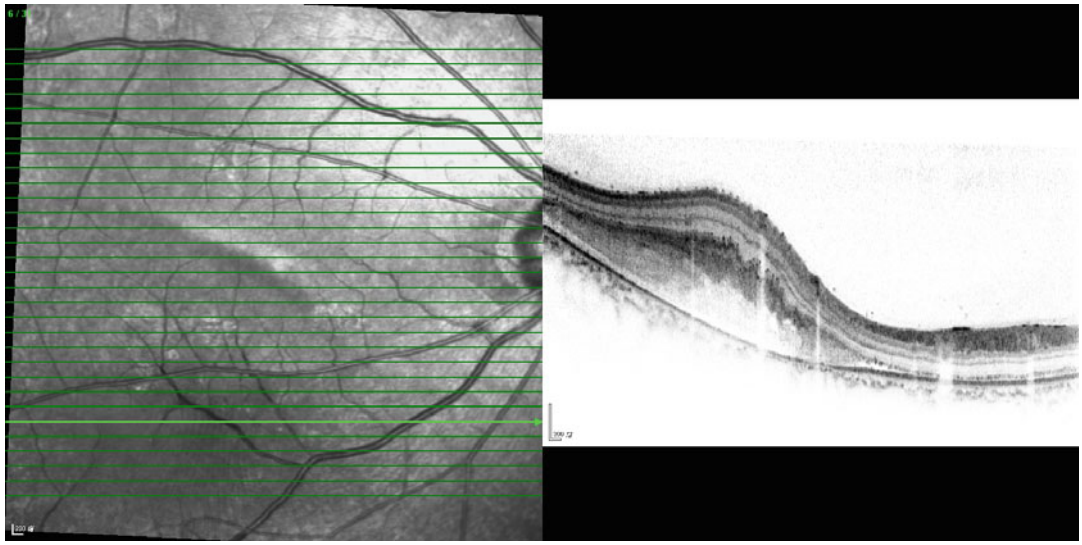

**Fig. 18.5** SD-OCT of the same eye with bullous central serous chorioretinopathy showing large amount of subretinal fluid with exudate showing as hyper-reflective material beneath the neurosensory retina

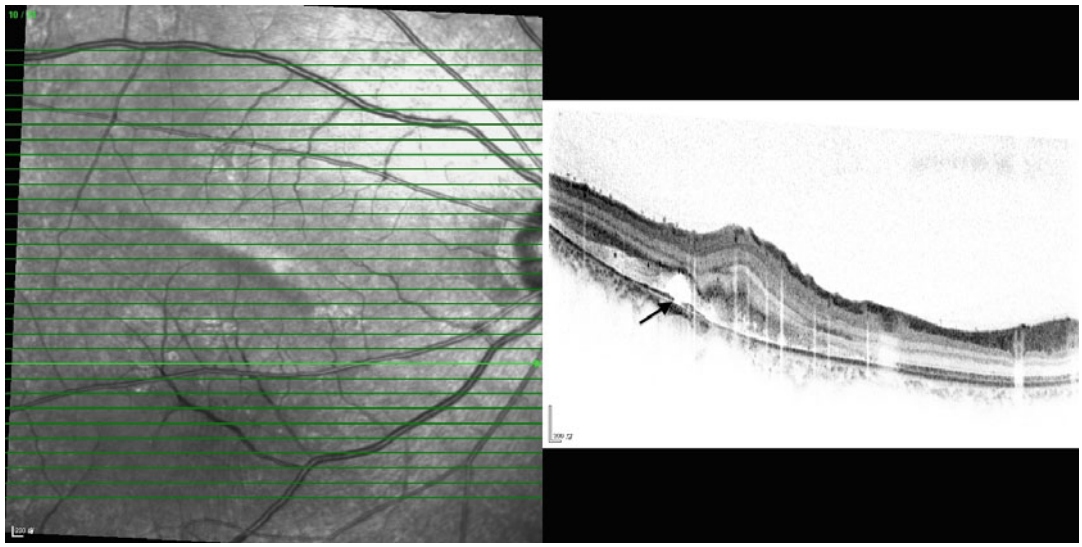

**Fig. 18.6** SD-OCT in an eye with bullous central serous chorioretinopathy showing RPE rip appearing as a defect in the RPE with a rolled edge

reflective dots, and RPE hypertrophy have all been shown to be associated with poor final visual acuity in eyes with resolved CSC (Matsumoto et al. 2009; Ozdemir and Erol 2013; Yalcinbayir et al. 2014) (Fig. 18.8). Therefore, periodic imaging with SD-OCT in eyes with CSC is useful in assessing the visual prognosis of these patients.

### 18.2.5 Subretinal Deposits in Central Serous Chorioretinopathy

Yellowish deposits forming a reticulated leopard spot pattern have been reported in eyes with chronic neurosensory detachment caused by CSC (Iida et al. 2002). These deposits can be found within the areas of neurosensory detachment and

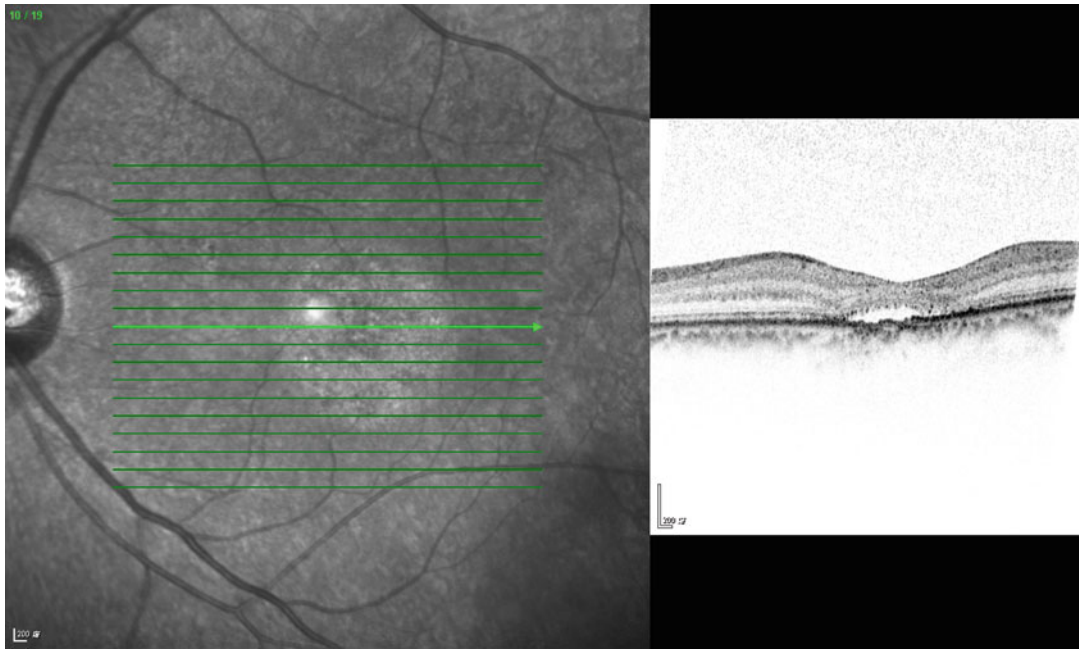

**Fig. 18.7** SD-OCT showing shallow subretinal fluid with subretinal hyper-reflective dots and granulated and partially thinned retina

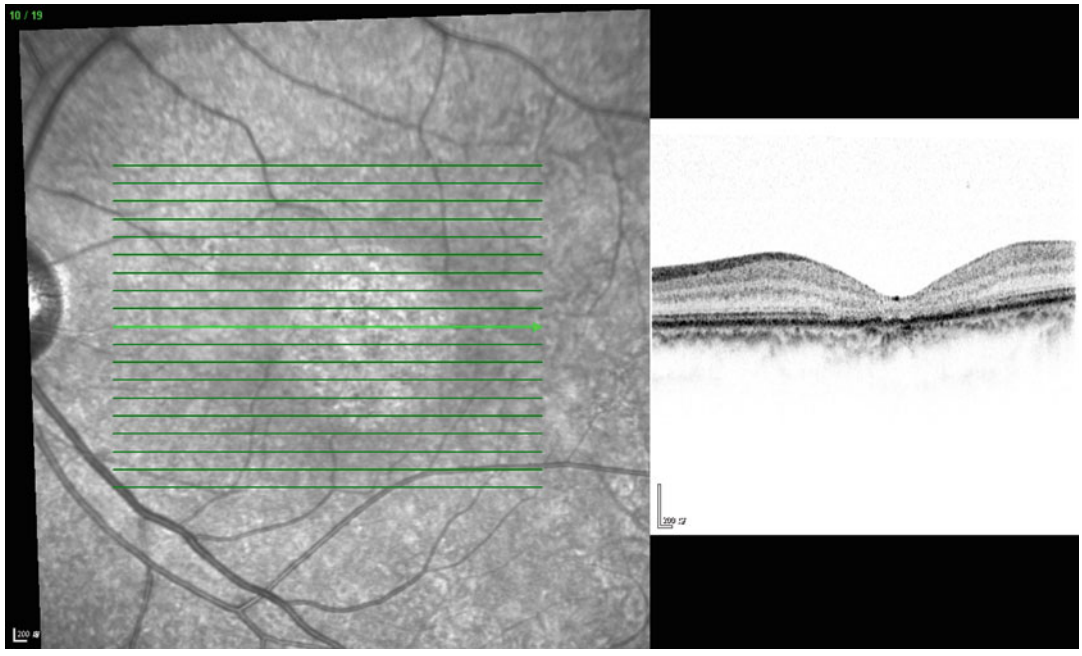

**Fig. 18.8** SD-OCT showing disruption of ellipsoid zone after complete resolution of subretinal fluid in chronic CSC

increase in size and amount with increasing duration of symptoms (Wang et al. 2005). SD-OCT imaging of these yellowish drusen-like granular deposits correlated well with the hyper-reflective deposits found on the posterior surface of the neurosensory retina as well as in the subretinal cavity (Fig. 18.9). It has been suggested that these deposits are composed of fragments of photoreceptor OS that accumulate when they were unable to be phagocytosed by RPE due to presence of neurosensory detachment, especially when the detachment is prolonged for over 4 months (Pryds and Larsen 2013). Other possible explanations for these deposits include plasma proteins extruded from the choriocapillaris, inflammatory debris, and lipid exudate originating from occult choroidal neovascularization secondary to CSC (Wang et al. 2005). Eyes with foveal subretinal deposit on presentation usually do not recover to the full functional and structural status compared with the asymptomatic fellow eyes even after complete resolution of the neurosensory retinal detachment following treatment with photodynamic therapy. This seems to indicate that the subretinal deposits are associated with irreversible foveal damage in CSC (Pryds and Larsen 2013).

### 18.2.6 Decrease in Outer Nuclear Layer (ONL) Thickness in Central Serous Chorioretinopathy

While the time-domain OCT allows visualization of the IS/OS junction with a resolution of up to 10 μm, the SD-OCT has an axial resolution of up to 1 μm, which enables visualization the external limiting membrane (ELM), in addition to showing the IS/OS line more clearly. The outer nuclear layer (ONL) represents the cell bodies of the cone photoreceptors. The outer limit of the ONL is the ELM, while at the central fovea, the inner boundary of the ONL almost abuts the internal limiting membrane (ILM). Matsumoto and colleagues defined the distance between the ILM and ELM at the fovea as the ONL thickness and evaluated this in patients with CSC (Matsumoto et al. 2009). Eyes were classified into two groups according to

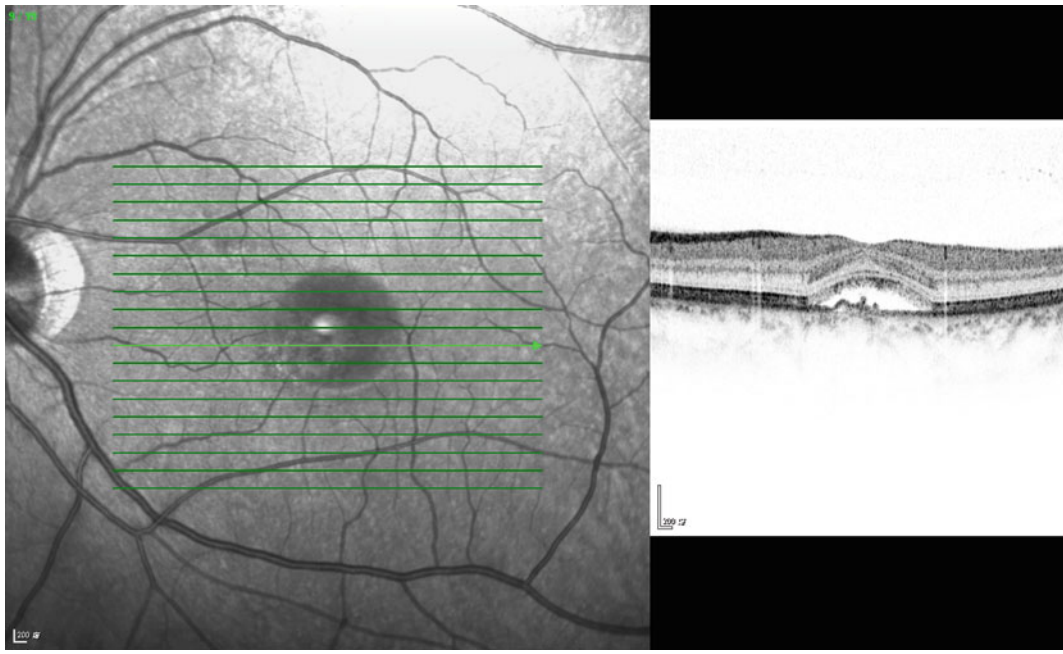

**Fig. 18.9** SD-OCT in an eye with chronic CSC showing subretinal fluid with hyper-reflective deposits on the posterior surface of the neurosensory retina and in the subretinal space

BCVA. Eyes with BCVA poorer than 20/20 were found to have significantly thinner ONL compared with those with BCVA better than 20/20, which in turn was significantly thinner than the ONL of normal controls. It was hypothesized that in serous retinal detachment, the retinal insults begin in the photoreceptor OS, where the disruption of the physiological phagocytosis of the OS by RPE cells leads to elongation of the OS, which eventually leads to apoptosis of photoreceptor cell bodies and thinning of the ONL. The thinning of central foveal thickness has been replicated in other studies (Kim et al. 2012; Ooto et al. 2010). The ONL reflects photoreceptor volume and was found to be a more sensitive indicator of visual outcome than IS/OS junction disruption (Ooto et al. 2010).

### 18.2.7 Retinal Pigment Epithelial Layer Changes and Pigment Epithelial Defect in Central Serous Chorioretinopathy

Morphological alterations of the RPE invariably occur at the point of angiographic leakage on FA in CSC. They can be shown on both cross-sectional and en face SD-OCT scans as PED, RPE irregularities, RPE bulge or protrusions (defined as an absence of an optically clear space within the lesion in contrast with PED), RPE hyperplasia, and RPE micro-rip (Gupta et al. 2010a; Kim et al. 2012; Lehmann et al. 2013; Shinojima et al. 2010).

PEDs are found in nearly all eyes with acute CSC. They are shown to persist in chronic CSC and in quiescent eyes even after resolution of SRF (Fujimoto et al. 2008; Song et al. 2012). Serous PEDs in SD-OCT are characterized by separation of the RPE (shown as a hyper-reflective line) from the underlying Bruch's membrane with an optically empty space in between. PEDs in acute CSC tend to be semicircular in shape with a smooth surface (Fig. 18.10), while those in chronic CSCs are usually low or flat with a dimpled or irregular surface (Song et al. 2012) (Fig. 18.11). It has been postulated that in CSC, the RPE overlying the hyperpermeable choroidal circulation is damaged from the exudation and becomes dysfunctional. The increased hydrostatic pressure from the choroidal circulation pushes the RPE forward and thereby creating a PED. A "micro-rip" or blow-out of the RPE can occur if the damage is severe, resulting in a focal leak which shows up as a leakage spot on fluorescein angiography (Fujimoto et al. 2008). These RPE micro-rips could be seen morphologically on SD-OCT scans (Kim et al. 2012). Once the fluid egresses from the sub-RPE space to the subretinal space, the pressure equalizes which causes the collapse of the PED. As the walls of the PED collapse, the RPE micro-rip may seal or bundle up appearing as RPE irregularities or hyperplasia on OCT (Gupta et al. 2010a, b; Shinojima et al. 2010). Once the RPE seals, the subretinal fluid will usually absorb leading to spontaneous CSC resolution.

Abnormalities in the RPE can be seen not only in eyes with active CSC but also in asymptomatic fellow eyes. Gupta and colleagues demonstrated that RPE bumps and PED could be seen in 94% and 12% of asymptomatic fellow eyes of CSC patients, respectively (Gupta et al. 2010b). The study provided evidence that CSC is a bilateral disease with asymmetrical clinical features. The RPE bumps may be related to underlying hyperpermeable choroid together with impaired RPE function leading to pooling of fluid in the sub-RPE space and might represent a preclinical or subclinical state of the disease. Yalcinbayir and colleagues noted that RPE bumps and hypertrophy were correlated with poor visual acuity, and the presence of these abnormalities on OCT may provide an indirect evidence of earlier photoreceptor damage and worse visual outcome (Yalcinbayir et al. 2014).

PED in CSC can also be visualized using en face OCT. They appear as circular with smooth inner silhouette on coronal section and are characterized by a hypo-reflective area surrounded by a well-defined hyper-reflective margin. PEDs tend to be located within or at the edge of serous retinal detachment (Lehmann et al. 2013). With the en face SD-OCT, RPE hyperplasia can be seen as a hyper-reflective area overlying the RPE

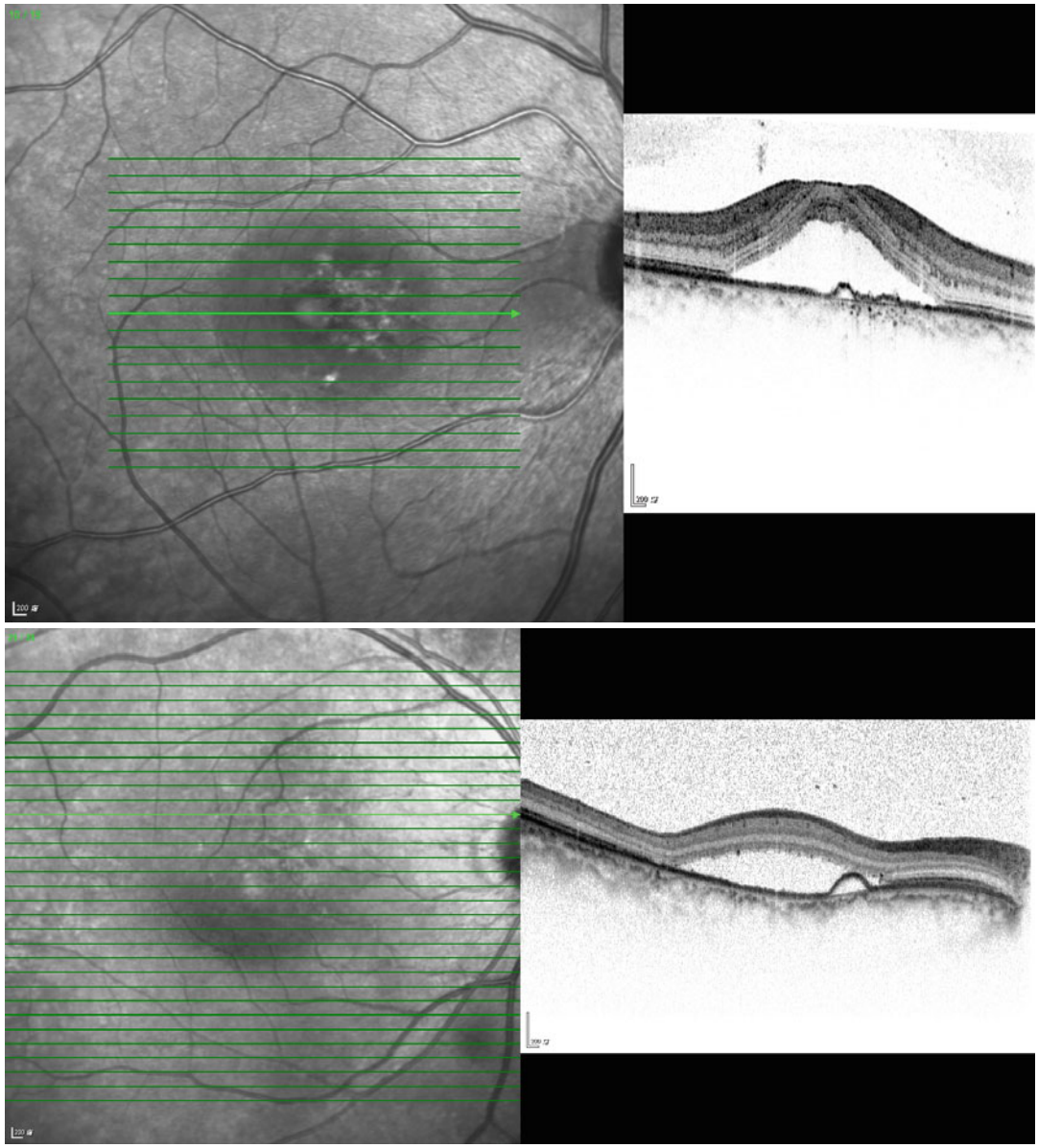

**Fig. 18.10** SD-OCT of an eye with acute CSC showing subretinal fluid with semicircular-shaped PED with smooth surface

in 31 % of eyes with CSC (Lehmann et al. 2013). These areas of RPE hyperplasia are often located with small PEDs over the leakage points on FA. Under the RPE abnormalities, they noted choroidal cavitations, shown as multiple black hypo-reflective cystic lesions corresponding to abnormal choroidal dilatations on transverse EDI-OCT scans.

### 18.2.8 Secondary Choroidal Neovascularization in Central Serous Chorioretinopathy

Choroidal neovascularization (CNV) can arise as a complication of CSC, as with any other lesions of the RPE or the Bruch's membrane. It occurs more frequently in chronic retinal

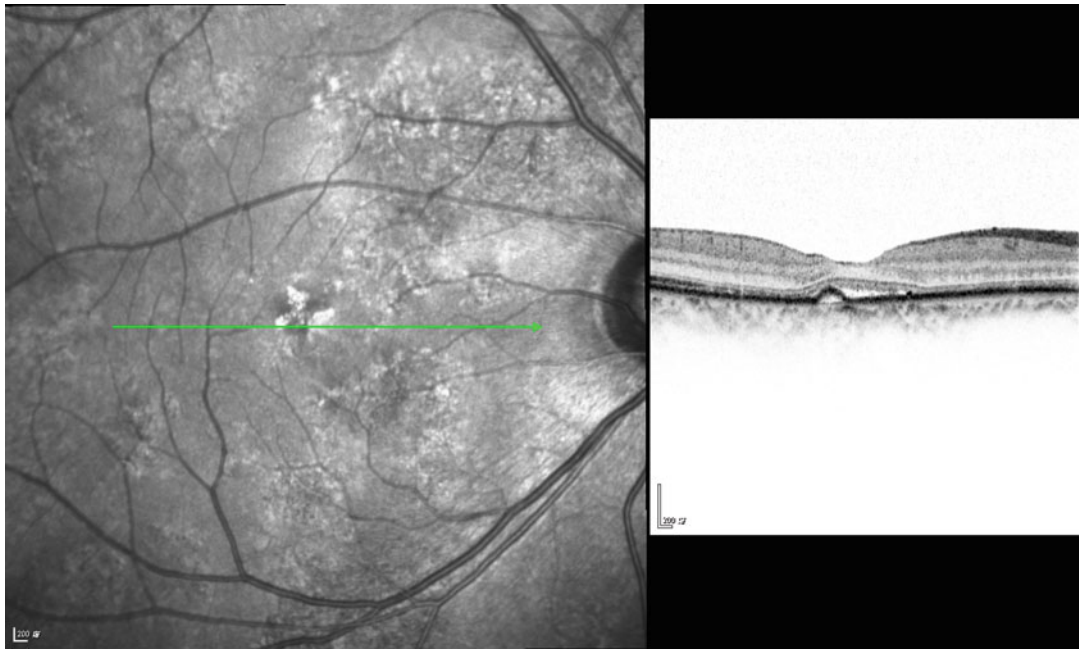

**Fig. 18.11** SD-OCT of an eye with chronic CSC showing subretinal fluid with semicircular-shaped PED with dimpled surface

pigment epitheliopathy and has a reported incidence of 4 % (Chan et al. 2003). CNV may occur after a long period after resolution of the acute disease and might be confused with CNV associated with age-related macular degeneration (AMD) in older patients (Wang et al. 2005). CNV in long-standing CSC are more likely to be type 2 membranes (Chan et al. 2003), but associations with type 1 CNV and polypoidal choroidal vasculopathy (PCV) have also been reported (Fung et al. 2012). Patients who have received laser photocoagulation for CSC can also develop laser-induced CNV, with a reported incidence from 0.6 to 5 % (Matsunaga et al. 1995).

The exact hypothesis of secondary CNV in CSC is unclear. It is hypothesized that in normal eyes, the Bruch's membrane acts as a barrier against CNV formation (Fung et al. 2012). In cases of CSC, chronic RPE decompensation or splitting of the RPE/Bruch's membrane complex in serous PEDs together with ischemic changes of the choriocapillaris may be factors leading to CNV development (Chan et al. 2003; Levine et al. 1989).

CNV in CSC typically has classic features of a well-delineated membrane in the early phase with intense leakage in the late phase on FA (Cooper and Thomas 2000). OCT shows a subretinal membrane associated with subretinal fluid (Fig. 18.12). Intravitreal anti-vascular endothelial growth factor (anti-VEGF) therapy such as bevacizumab and ranibizumab has been investigated and appeared to be a useful treatment modality, with OCT resolution or reduction of the subretinal fluid and shrinkage of the CNV membrane (Konstantinidis et al. 2010; Montero et al. 2011; Nomura et al. 2012) (Fig. 18.13).

### 18.2.9 Enhanced Depth Imaging for Choroidal Changes in Central Serous Chorioretinopathy

*Choroidal Thickness* Imamura and colleagues (Imamura et al. 2009) demonstrated using EDI-OCT imaging that the subfoveal choroidal thickness was increased in both acute and chronic cases of CSC (Fig. 18.14). In the study, the mean

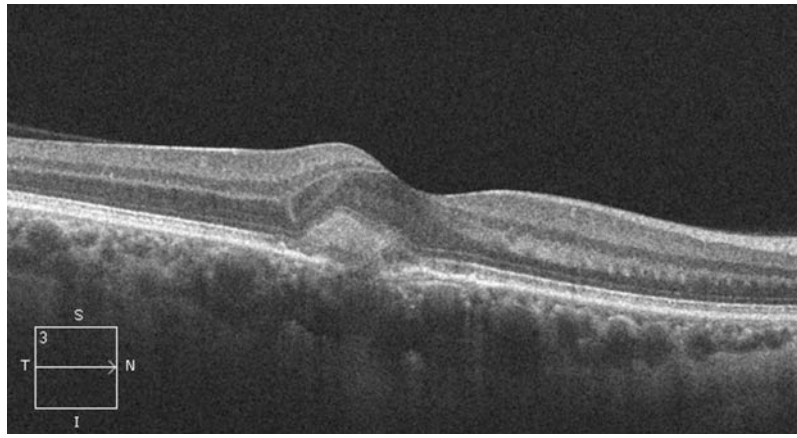


**Fig. 18.12** SD-OCT of an eye with a history of CSC showing hyper-reflective lesion at the RPE level due to CNV formation

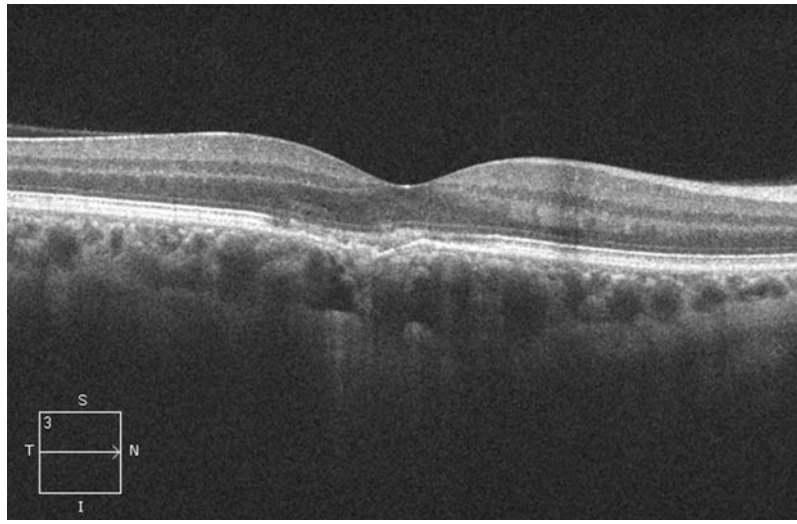


**Fig. 18.13** SD-OCT after intravitreal anti-VEGF therapy for CNV secondary to CSC showing complete resolution of fluid and regression of the CNV

choroidal thickness was greater in eyes with CSC compared with normal eyes by a mean of 214 μm. The results provided evidence that there is expansion of the choroid as a result of the venous dilatation and increased hydrostatic pressure in the choroid in eyes with CSC.

*Choroidal Vessels* EDI-OCT imaging can be performed simultaneously with ICGA. Yang and colleagues showed that in the ICGA hyperfluorescent areas, there was reduction in hyperreflectivity beneath Bruch's membrane on EDI-OCT, suggesting thinning of the small to medium vessel layers of the choroid (Yang et al. 2013). Underneath this thinned layer, enlarged, hypo-reflective (similar to subretinal fluid) lumina were identified, suggesting dilatation of the large choroidal vessels. The diameters of the hypo-reflective choroidal lumina in hyperfluorescent ICGA areas were significantly associated with increased subfoveal choroidal thickness. They suggested interstitial edema may play a role in addition to choroidal dilatation.

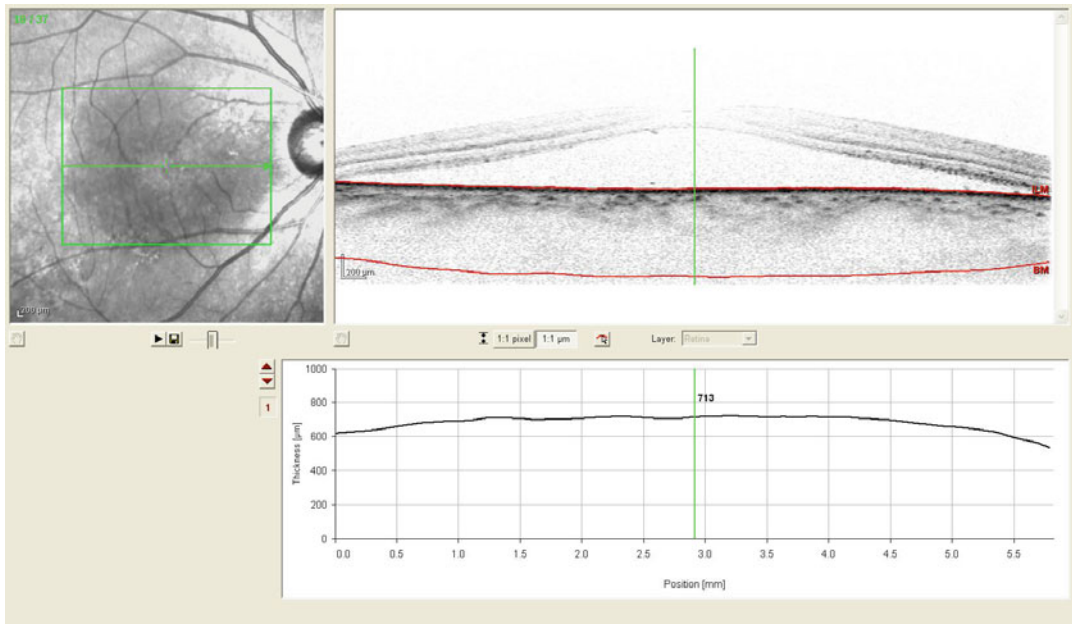


**Fig. 18.14** EDI-OCT showing subretinal fluid with increased choroidal thickness in acute CSC

*RPE Layer Changes* A "double-layer sign" can be seen on EDI-OCT scans, most often in chronic CSC eyes where the RPE layer has an undulated non-dome-shaped appearance, while the underlying intact Bruch's membrane appears as a straight line. The space in between the double layer could either be hyper- or hypo-reflective, but hyporeflectivity is seen in the majority of CSC eyes. This feature can also be found in eyes with PCV, where the space is hyper-reflective in most eyes with PCV. This can be used as one of the distinguishing features between the two diseases. It has been postulated that the difference in the reflectivity between eyes with PCV and CSC may be due to differences in the hyperpermeability of the choroidal vessels between the two diseases (Yang et al. 2013).

In both acute and chronic CSC, RPE hyperplasia that corresponds to focal leak on FA could be seen and can act as a guide to localize treatment area. Choroidal cavitation, defined as multiple, black hypo-reflective cystic lesions, could be seen in en face OCT at a layer just beneath the choriocapillaris, situated in areas of abnormal RPE. This could represent ischemic choroidal areas around focal hyper-fluorescent spot observed on FA (Lehmann et al. 2013).

### 18.2.10 Focal Choroidal Excavation in Central Serous Chorioretinopathy

Focal choroidal excavation (FCE) is a localized trough within the submacular choroid, along the RPE/Bruch's membrane complex line seen on SD-OCT scans. On fundus examination, FCE appears as mild pigmentary mottling or a small yellowish spot, which can only be confirmed with OCT imaging. It can be classified as conforming, if the photoreceptor tips are attached to the apical surface of the RPE (Fig. 18.15), or nonconforming if the photoreceptor tips and the RPE are separated (Fig. 18.16). Eyes with nonconforming type are generally more visually symptomatic as patients may develop metamorphopsia or blurred vision. FCE can also be classified in terms of its location: foveal if the foveal center is within the choroidal excavation or extrafoveal if the foveal center is not within the excavation.

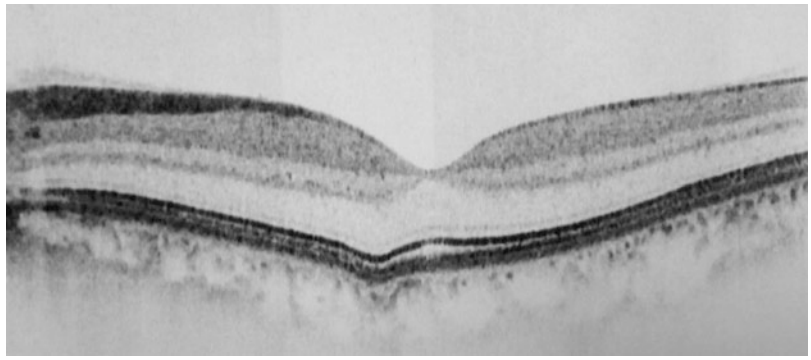

**Fig. 18.15** SD-OCT of an eye with focal choroidal excavation showing photoreceptor layer is attached to the apical surface of the RPE in the excavation

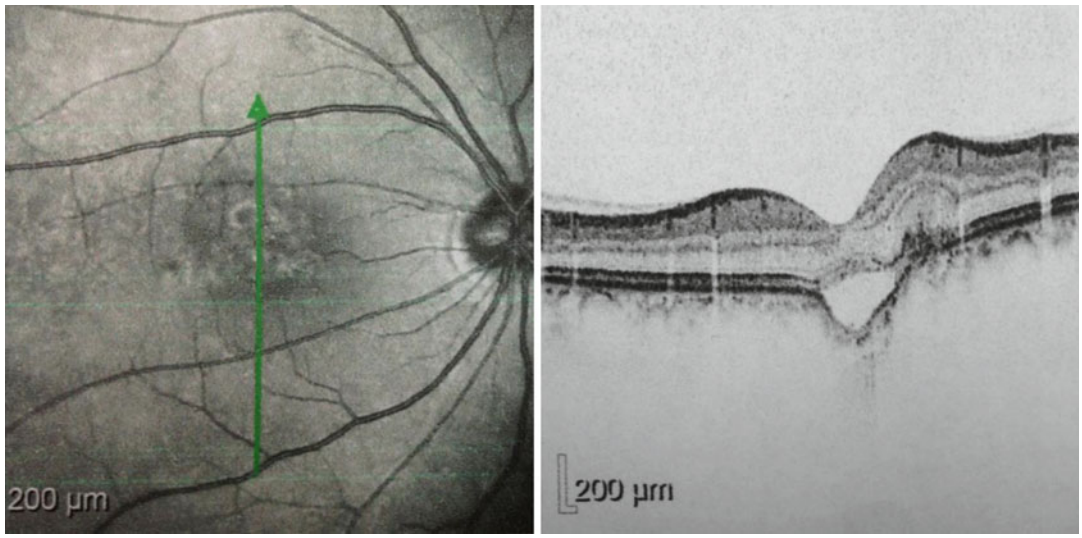


**Fig. 18.16** SD-OCT of an eye with focal choroidal excavation showing photoreceptor layer is separated from the apical surface of the RPE in the excavation

While FCE was first reported in normal eyes, it is more commonly found in association with other macular diseases such as PCV and CNV (Lee and Lee 2014). In a small case series, FCE was found to be present in around 8 % of eyes with CSC, especially in myopic eyes (Ellabban et al. 2013). It is unclear whether FCE is a congenital or acquired condition, but FCE tends to remain unchanged over time. There are close topographic associations between FCE and CNV/PCV. It has been suggested that anatomic alterations or relative choroidal ischemia at the excavation site due to focal thinning could predispose FCE eyes to develop CNV at the excavated area (Lee and Lee 2014). FCE is often found to be within or next to leakage points seen in FA (Ellabban et al. 2013; Suzuki et al. 2014). Choroidal vascular hyperpermeability was found in nearly all eyes around the FCE or in a wide area outside the FCE (Luk et al. 2015). It remains unknown whether FCE plays a pathogenic role in the development of CSC.

En face SD-OCT imaging at the level beneath the FCE has shown unusual choroidal tissue devoid of normal large choroidal vessels bridging

between the bottom of the excavation and the outer choroidal boundary (Ellabban et al. 2013). In some eyes, the outer boundary of the choroid seemed to be pulled inward, showing the underlying suprachoroidal space. This suggests a focal scarring process might be involved resulting in focal retraction of the RPE with FCE formation. This finding is supported by later studies where this hyper-reflective band was found in 54 % of eyes with FCE (Lee et al. 2014). This hyper-reflective layer was found to be associated with decreased choroidal thickness which further supports the theory that there is scarring and contraction of choroidal tissue in the development of FCE.

## 18.3 Correlation of SD-OCT Findings with Other Imaging Modalities

### 18.3.1 Fundus Autofluorescence

Fundus autofluorescence (FAF) is an imaging technique that reflects the intensity and spatial distribution of autofluorophores in the retina. The main autofluorophore is pyridinium bisretinoid (AE2), contained in lipofuscin which is a breakdown product of phagocytosed photoreceptor OS. When stimulated by light of specific wavelengths, autofluorophore emits light which can be captured by imaging systems focusing on the RPE.

In acute CSC, there may be no abnormal FAF findings until after several months, when diffuse hyper-autofluorescence develops along the inferior border of the retinal detachment. This is due to buildup of autofluorescent materials in the subretinal space caused by impaired phagocytosis of the photoreceptor OS. There may also be small punctate hyper-autofluorescence, resulting in a granular appearance. These precipitates are common and can appear in up to 65 % of eyes with CSC (Maruko et al. 2011a). They correspond to hyper-reflective lesions in the outer retina or subretinal space in SD-OCT scans. It has been hypothesized that the precipitates could be accumulations of shed photoreceptor outer segments or engorged macrophages that have phagocytosed them (Nicholson et al. 2013).

In chronic CSC, there are often FAF changes that reflect large areas of RPE atrophy or damage. Gravity-driven descending tracts of subretinal fluid can be seen. These tracts appear hyper-autofluorescent when the fluid first occurs, then becoming increasingly hypo-autofluorescent as the underlying RPE is damaged in the path of the fluid. Imamura and colleagues classified hypo-autofluorescence in CSC into granular or confluent types (Imamura et al. 2011). They noted the granular type seemed to signify incomplete loss of RPE cells and therefore appeared as intermixed dots of normal autofluorescence and hypo-autofluorescence in between, while confluent type appears as a uniform hypo-autofluorescence, indicating confluent cell loss. This could be correlated with OCT scans where areas of hypo-autofluorescence on FAF are associated with atrophy of the RPE and the outer retina, as well as photoreceptor damage seen as IS/OS disruption on OCT scans (Spaide et al. 2008; Kim et al. 2013). The presence of granular or confluent hypo-autofluorescence at the macula or peripapillary area or descending tract from the macula has been shown to be a significant predictor for poor visual acuity.

Recent developments in autofluorescence imaging have used infrared (IR) or near-IR autofluorescence as the stimulating light source instead of the traditional short wavelength (SWL) autofluorescence. In these FAF images, melanin is the main autofluorophore, in contrast to lipofuscins in SWL autofluorescence. Granular hyper-IR autofluorescence was noted in CSC that changed to hypo-autofluorescence later in the disease course and is hypothesized to be due to modification of melanin in the RPE. Also, areas of simultaneous punctate hyper-IR autofluorescence and hyper-SWL autofluorescence could be seen. These areas correspond to RPE hyperplastic areas on OCT scans and are speculated to be hyperplastic RPE clumps (Sekiryu et al. 2010; Kim et al. 2013).

### 18.3.2 Fluorescein Angiography

Fluorescein angiography (FA) is widely used in the diagnosis and treatment of CSC. In acute CSC, the most characteristic feature is one or more expanding dots of fluorescein that pools in the serous retinal detachment. The classic "smokestack" appearance, where the dye rises from the leakage point to the top of the neurosensory detachment then spreads laterally due to osmotic gradient between old and new fluid within the detachment, is less commonly seen than the inkblot or mushroom-shaped dye pattern. The pinpoint leak on FA represents leakage of dye from the choroid through a focal RPE defect which is present in about 95 % of CSC cases. The leak is usually within 1500 μm of the fovea, most commonly in the supero-nasal quadrant as gravity pulls the fluid inferiorly (Ross et al. 2011).

Correlation of FA leakage points with cross-sectional SD-OCT scans shows RPE abnormalities in nearly all eyes. PEDs are present in 61–71 % of eyes, while a protruding or irregular RPE layer is seen in 32–100 % (Fujimoto et al. 2008; Kim et al. 2012; Shinojima et al. 2010). SD-OCT enables the detection of small or shallow PEDs which cannot be detected on FA alone. RPE micro-rips or defects within these PEDs or RPE irregularities have been matched precisely to leakage points on FA and provide further evidence that RPE abnormalities are involved in the pathogenesis of CSC (Kim et al. 2012). On follow-up assessment, these RPE rips undergo spontaneous closure, replaced by RPE hypertrophy (Gupta et al. 2010a).

In multifocal or chronic CSC, multiple areas of pinpoint leakage and neurosensory detachment filling could be seen. As the RPE is damaged from repeated neurosensory detachment and SRF, hyper-fluorescent window defects could be seen, often along gravitational tracts corresponding to areas of RPE atrophy. SD-OCT imaging of these window defects shows different degree of damage to the RPE or the outer retina including the IS/OS junction and the external limiting membrane (Kim et al. 2013).

### 18.3.3 Indocyanine Green Angiography

The use of indocyanine green angiography (ICGA) has shed much light on the pathophysiology of CSC. It is also used to guide treatment with verteporfin photodynamic therapy (PDT). Characteristically, ICGA shows initial hypofluorescence with delayed choroidal arterial filling, followed by mid-phase hyperfluorescence due to vascular hyperpermeability and late-phase washout of indocyanine green dye (Ross et al. 2011; Quin et al. 2013). It is suggested that the initial delayed arterial filling is due to choroidal capillary and venous congestion, as leakage from RPE on FA only occurs in areas where ICGA showed delayed arterial filling (Kitaya et al. 2003). Localized hyperfluorescence suggests areas of underlying choroidal hyperpermeability and dilatation.

With the use of en face EDI-OCT, it was demonstrated that areas of dilation of choroidal vascular network corresponded exactly with the choroidal abnormalities in ICGA. In contrast to hyperfluorescence on ICGA, dilated choroidal vessels show up as large hypo-reflective tubes in an interconnected network on en face EDI-OCT (Lehmann et al. 2013). Ferrara and colleagues further characterized these dilatations as focal or diffuse choroidal dilation (Ferrara et al. 2014). Dilatations are considered as focal if some vascular branches have larger caliber than the surrounding branches and as diffuse if the dilatations are relatively homogeneous. The areas of dilatation corresponded to areas of choroidal hyperperfusion on ICGA and are invariably found in eyes with overlying PED or RPE changes. En face EDI-OCT may be more advantageous than ICGA in assessing choroidal vessel dilatation as it can provide cross-sectional information about the choroidal vasculature in individual layers (choriocapillaris, Sattler's and Haller's layer could be separately analyzed), whereas in ICGA, all the layers are compressed into a two-dimensional image. In addition, en face OCT is noninvasive and can provide the same information on the choroidal vasculature using ICGA (Ferrara et al. 2014).

**Table 18.1** Comparisons of OCT findings of macular disorders which might resemble CSC

| OCT feature | Central serous chorioretinopathy | Polypoidal choroidal vasculopathy | Serous PED in AMD | Vogt-Koyanagi-Harada disease |
|---|---|---|---|---|
| Intraretinal fluid | Usually mild or minimal | Present | Present | Mild intraretinal cyst in acute phase |
| Subretinal fluid | Marked in acute phase | Mild | Mild | Marked in acute phase<br>Can occur in multiple pockets |
| RPE level | Double-layer sign with hypo-reflective space.<br>Circular PED | Double-layer sign with hyper-reflective space due to branching vascular network<br>Sharp protrusion of RPE layer due to polyp | Irregular due to drusen or RPE atrophy | Undulations due to infiltration of inflammatory cells |
| EDI-OCT choroidal layer | Increased choroidal thickness<br>Small- and medium-sized vessel thinning | Increased choroidal thickness | Reduced choroidal thickness | Increased choroidal thickness in acute phase<br>Small- and medium-sized vessel thinning<br>Dilation of large choroidal vessels |
| En face OCT | PED with smooth inner silhouette, uniform borders, and clear content | Branching vascular network | PED has irregular borders | N/A |

## 18.4 Use of SD-OCT to Differentiate Other Conditions Mimicking Central Serous Chorioretinopathy (Table 18.1)

### 18.4.1 Polypoidal Choroidal Vasculopathy

Polypoidal choroidal vasculopathy (PCV) was first described by Yannuzzi in 1982. It is now considered a subtype of neovascular AMD which is characterized by aneurysmal or polyp-like abnormalities with a branching vascular network (BVN) of neovascularization in the inner choroidal vessels seen on ICGA. It typically shows multiple, recurrent serosanguineous detachment of the retina and RPE with leakage and bleeding from the polypoidal lesions or BVN (Ciardella et al. 2004). There are some similarities between PCV and chronic CSC which might lead to misdiagnosis of chronic CSC patients as having PCV and vice versa. Both diseases tend to occur in patients with younger age than typical AMD, and both conditions are associated with multifocal choroidal vascular hyperpermeability on ICGA, increased choroidal thickness, and dilated thin-walled choroidal vessels histologically (Mrejen and Spaide 2013; Sasahara et al. 2006). It has been suggested that chronic CSC may predispose to formation of polypoidal lesions and maybe an ocular risk factor for PCV (Koizumi et al. 2013; Sasahara et al. 2006). However, PCV is more commonly associated with subretinal exudation, fibrin deposition, and hemorrhages which generally leads to a poorer visual outcome.

OCT studies of eyes with PCV show sharp protrusions of the RPE correlating to orange red nodules seen clinically (Fig. 18.17). A characteristic "double-layer sign" consisting of a two lines at the RPE level with hyper-reflective material in between could be seen in PCV, and this is considered to correspond to the BVN (Sato et al. 2007). In CSC, although a similar double-layer sign could be seen, the space between the two layers is usually hypo-reflective (Yang et al. 2013).

Cystoid macula edema, lipid deposits, subretinal hemorrhage, and hemorrhagic PED are more commonly seen in PCV but not CSC (Ooto et al. 2011). In the retina, the thickness of the outer nuclear layer as well as the inner segment of the photoreceptor is decreased in both PCV and CSC, which correlates with poor visual acuity. However, in PCV, the thickness of the photoreceptor OS is thinner than normal individuals, while in CSC, the OS is similar or thicker than normal individuals (Ooto et al. 2010). Elongation of OS could be seen in CSC, but it is rare in PCV. This suggests that photoreceptors may be more severely damaged by the subretinal fluid in PCV than CSC, which often contains fibrin or hemorrhage. This leads to poorer visual outcome in PCV than CSC (Kim et al. 2012; Matsumoto et al. 2009; Ooto et al. 2010).

### 18.4.2 Serous Pigment Epithelial Detachment in Age-Related Macular Degeneration

The diagnosis of CSC can sometimes be confused with AMD, especially in cases of chronic CSC among older patients. Overlapping features of the two conditions include chronicity, RPE hyperplasia or atrophy, PED, subretinal fluid, cystoid macular degeneration, retinal atrophy, and hyperfluorescence on FA or ICGA (Fung et al. 2012). There are several ways to differentiate the two diseases using SD-OCT imaging. In CSC, the PED tends to be smaller and more circular and have a clear content (Cho et al. 2010). Subretinal fluid and hypertrophic outer retinal changes are more common in CSC than in AMD, but there is less intraretinal fluid in CSC compared with AMD (Lumbroso et al. 2011). On EDI-OCT imaging, choroidal thickness is usually increased in CSC, whereas the choroidal thickness is typically reduced in AMD. With en face OCT imaging, PEDs in CSC are circular with smooth inner silhouette, clear contents, and uniform borders, where the borders are often irregular in AMD. The OCT findings, combined with medical history (eg, steroid use), demographics (eg, younger patient), other clinical features (eg, absence of drusen), and features of other investigations (eg, bilateral vascular hyperpermeability on mid-phase ICGA), often enable clinicians to differentiate among these two disease entities.

### 18.4.3 Vogt-Koyanagi-Harada Disease

Vogt-Koyanagi-Harada (VKH) disease is an idiopathic granulomatous inflammatory disorder that affects the eyes, meninges, and skin. The main site of the intraocular inflammation is the choroid. The clinical course of VKH disease is divided into acute, chronic, and convalescent stages. Eyes during acute VKH disease stage are characterized by bilateral multifocal serous neurosensory detachments. In the convalescent stage, the retinal detachment resolves and develops late manifestations such as ocular depigmentation, peripheral nummular scars, pigmentary changes of the RPE, or recurrent chronic anterior uveitis.

VKH can sometimes be confused with CSC, especially in the acute stage where both conditions present with neurosensory retinal detachment. Differentiating between the two disease entities is important as VKH is treated with high-dose steroids while CSC is aggravated by steroid therapy. Characteristic FA findings for VKH disease include disseminated spotted choroidal hyperfluorescence and multifocal pockets of SRF with pooling of dye and with disc leakage, while CSC typically present with inkblot or smokestack leakage patterns, and the SRF is mainly limited to the posterior pole with no disc leakage.

Using SD-OCT, differentiating features for VKH from CSC include large wavy undulations of the RPE, presence of subretinal septa, and intraretinal cystic space (Vasconcelos-Santos et al. 2010). In acute VKH disease, intraretinal cystic spaces corresponded to areas of dye pooling on FA. The retina is split just above the IS/OS junction in these cystic structures, and a membranous structure, represented by a highly reflective line, is seen at the floor of these cysts and is continuous with the IS/OS line (Ishihara

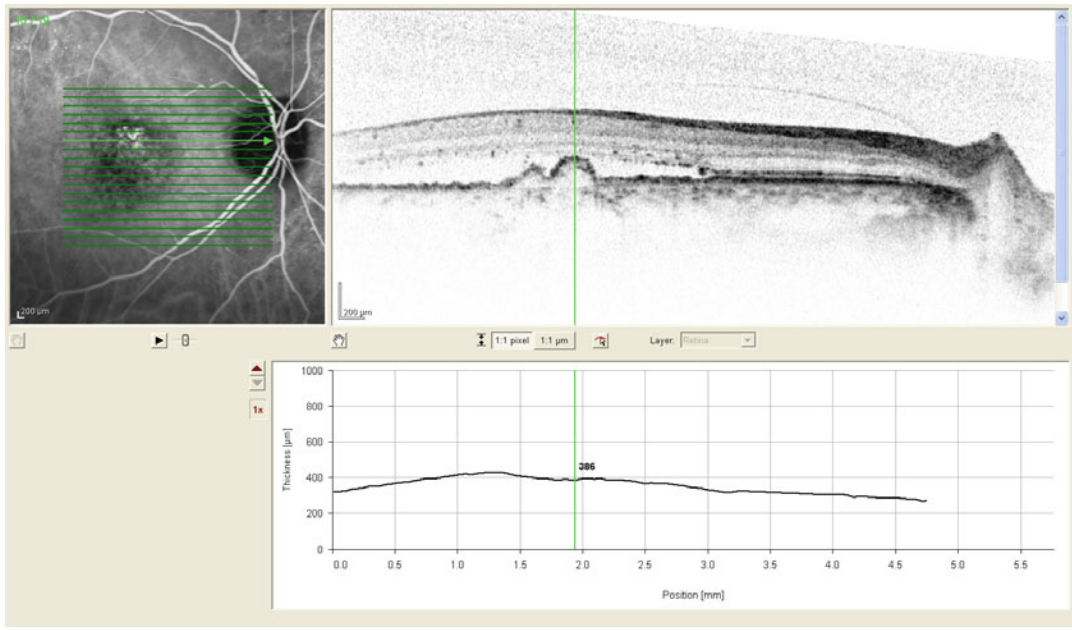


**Fig. 18.17** SD-OCT showing subretinal fluid with nodular protrusions at the RPE level due to polypoidal choroidal vasculopathy corresponding to the nodular hyperfluorescence as seen in ICGA

et al. 2009). Ishihara and colleagues hypothesized that inflammatory products such as fibrin binds to a portion of the OS layer and is split from the IS in these cystoid spaces (Ishihara et al. 2009). In areas of serous retinal detachment, irregularity of the IS/OS junction could be seen. Characteristic wavy undulations of the RPE can often be found in areas adjacent to the serous retinal detachment, probably representing areas of infiltration of inflammatory cells in the choroid and choroidal folds (Gupta et al. 2009).

In the chronic or convalescent phase of VKH disease, SD-OCT imaging of the hypopigmented atrophic lesions in sunset glow fundi shows RPE loss with variable involvement of the outer retinal layers. RPE thickening suggesting RPE hypertrophy could be seen in areas with pigmented or disciform scars.

EDI-OCT imaging of eyes with acute VKH disease shows diffuse choroidal thickening compared with convalescent phase VKH (Fong et al. 2011; Montero et al. 2011). Localized thickening of the choroidal compartment with subsequent bulging of the RPE/Bruch's reflective complex anteriorly ("choroidal bulging") has been observed in convalescent VKH, and this might suggest ongoing subclinical inflammation (Sakata et al. 2014).

Fong and colleagues demonstrated a loss of inner choroidal hyper-reflective foci in VKH patients in both acute and convalescent stages using EDI-OCT imaging (Fong et al. 2011). It was hypothesized that these hyper-reflective foci represent pericapillary arterioles and venules, which were damaged by inflammation and caused stromal shrinking and small vessel drop-out as shown on EDI-OCT. This hypothesis was later supported by further SD-OCT studies which showed loss of choriocapillaris layer in convalescent phase VKH, represented as a break in the hypo-reflective band just below the RPE/BM layer (Nazari et al. 2014). Eyes with CSC also showed a relative thinning of the inner choroidal layer of small- and medium-sized vessels. However, underneath the thinned inner choroidal layer, there is a relative dilation of the large choroidal vessels, shown as hypo-reflective lumina beneath the thinned inner choroidal layer, which contrasts with eyes with VKH disease (Yang et al. 2013).

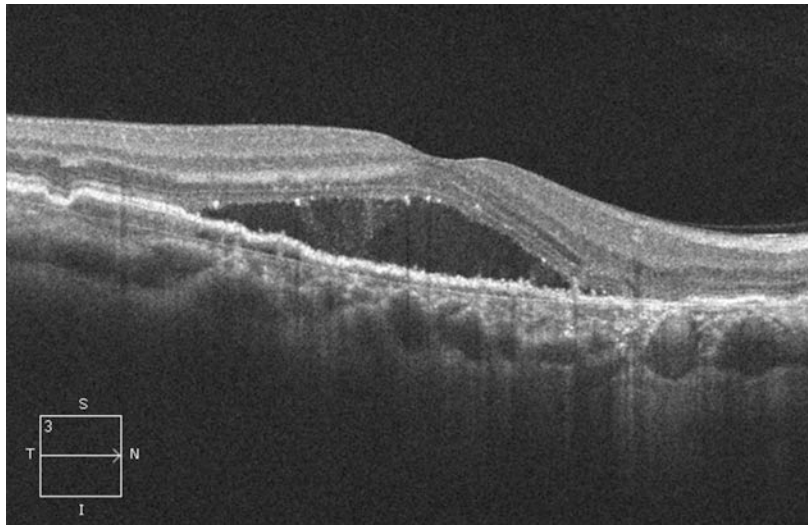


**Fig. 18.18** SD-OCT showing subretinal fluid in CSC prior to photodynamic therapy with half-dose verteporfin

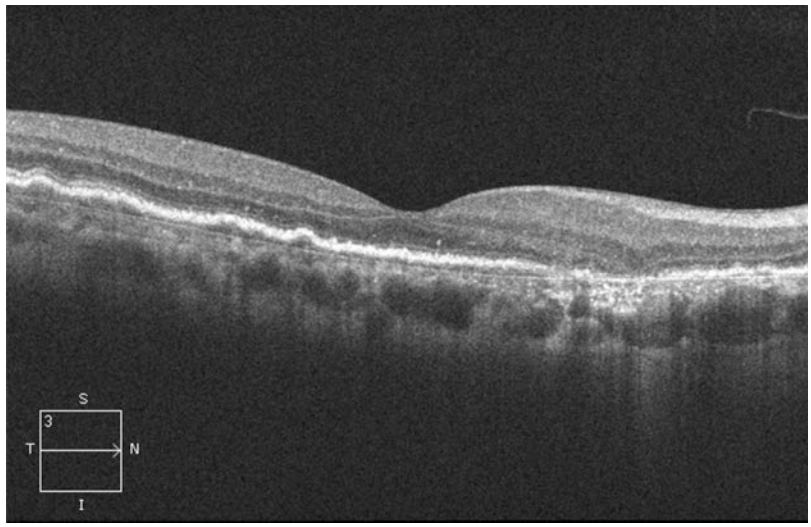


**Fig. 18.19** SD-OCT 1 month after photodynamic therapy with half-dose verteporfin showing complete resolution of subretinal fluid

## 18.5 Use of SD-OCT for Treatment Monitoring in Central Serous Chorioretinopathy

### 18.5.1 Photodynamic Therapy

Verteporfin PDT is useful in promoting resolution of acute and chronic CSC as well as to prevent recurrences. It causes remodeling of the choroidal vasculature and reduces choroidal hyperpermeability and congestion thereby addressing the root cause of the disease. Early reports using standard protocol PDT for CSC reported 60–100 % success rates with improvement of visual outcome in both acute and chronic cases (Yannuzzi et al. 2012). However, potential problems including foveal RPE atrophy, choroidal ischemia, and secondary CNV were reported to occur with standard PDT. More recently safety enhanced PDT, either

with reduced dose or fluence PDT, has been investigated with good results.

Chan and colleagues (Chan et al. 2008) performed a randomized control trial with half-dose verteporfin PDT for acute CSC eyes and found 95 % resolution of SRF in patients in the treatment group compared with 58 % in the placebo group. Reduced fluence, either by decreasing treatment time or energy output, was also found to be efficacious in speeding up subretinal fluid resolution with reduced complications such as CNV and choriocapillaris nonperfusion (Reibaldi et al. 2010).

SD-OCT imaging is useful in monitoring CSC following PDT in two ways. Firstly, it can monitor the height of serous retinal detachment following PDT and can detect any residual fluid that is not obvious on clinical examination (Figs. 18.18 and 18.19). Some eyes show a transient increase in exudation immediately following PDT, similar to eyes with CNV treated with PDT, with subsequent resolution of the subretinal fluid (Rogers et al. 2002). Secondly, by using EDI-OCT, subfoveal choroidal thickness can be assessed following PDT. Maruko and colleagues reported reduction of mean choroidal thickness from a baseline of 462 μm to 360 μm in PDT-treated eyes after 1 month, and ICGA showed decreased hyperpermeability (Maruko et al. 2010). This reduction was not seen in eyes treated with thermal laser photocoagulation.

### 18.5.2 Thermal Laser Photocoagulation

Conventional laser treatment for CSC is performed in CSC to obtain a confluent coagulation of moderate intensity covering the leakage point on FA. It is used to expedite the absorption of SRF in acute and chronic CSC, but it does not prevent recurrence (Nicholson et al. 2013). The exact mechanism of action for thermal laser in CSC is unclear, but it may cause direct sealing of the RPE leaking sites or by promoting RPE pumping function. Possible side effects include scotoma and late development of CNV, and therefore it is mainly used in chronic or refractory cases. However, it does not have a role in bullous variant of CSC (Liegl and Ulbig. 2014). Using SD-OCT to evaluate the photoreceptors before and after laser treatment in acute and chronic CSC, Odrobina and colleagues found that permanent damage to the photoreceptor layer and external limiting membrane occurred in 93 % of chronic CSC eyes but not in acute CSC eyes up to 12 months post-laser treatment and absorption of subretinal fluid (Odrobina et al. 2013). Changes include disruption of the foveal photoreceptor layer and external limiting membrane, persistent hyper-reflective subretinal deposits, and a noticeable RPE bulge, reflecting outer segment apoptosis and phagocytosis by RPE. This seems to indicate that early laser treatment of CSC results in quicker resolution of SRF and might reduce long-term photoreceptor damage and visual acuity loss.

While traditional laser is useful to shorten duration of serous detachment in CSC, it is not appropriate for juxtafoveal or subfoveal leakage points (leakage sites should be more than 375 μm from the fovea). A modified laser therapy with micropulse diode laser has been recently investigated, which involves applying a sub-threshold laser burn using a 810 nm diode laser to the leakage site, which leads to early resolution of serous retinal detachment in chronic CSC without leaving any visible scars on fundoscopy or on FA (Lanzetta et al. 2008; Roisman et al. 2013).

## References

Ahn SE, Oh J, Oh JH et al (2013) Three-dimensional configuration of subretinal fluid in central serous chorioretinopathy. Invest Ophthalmol Vis Sci 54:5944–5952

Bajarborua D (2001) Long-term follow-up of idiopathic central serous chorioretinopathy without laser. Acta Ophthalmol Scand 79:417–421

Castro-Correia J, Coutinho MF, Rosas V et al (1992) Long term follow up of central serous retinopathy in 150 patients. Doc Ophthalmol 81:379–386

Chan WM, Lam DS, Lai TY et al (2003) Treatment of choroidal neovascularization in central serous chorioretinopathy by photodynamic therapy with verteporfin. Am J Ophthalmol 136:836–845

Chan WM, Lai TY, Lai RY et al (2008) Half-dose verteporfin photodynamic therapy for acute central serous chorioretinopathy: one-year results of a randomized controlled trial. Ophthalmology 115:1756–1765

Cho M, Athanikar A, Paccione J et al (2010) Optical coherence tomography features of acute central serous chorioretinopathy versus neovascular age-related macular degeneration. Br J Ophthalmol 94:597–599

Ciardella AP, Donsoff IM, Huang SJ et al (2004) Polypoidal choroidal vasculopathy. Surv Ophthalmol 49:25–37

Cooper BA, Thomas MA (2000) Submacular surgery to remove choroidal neovascularization associated with central serous chorioretinopathy. Am J Ophthalmol 130:187–191

Ellabban AA, Tsujikawa A, Ooto S et al (2013) Focal choroidal excavation in eyes with central serous chorioretinopathy. Am J Ophthalmol 56:673–683

Fawzi AA, Holland GN, Kreiger AE et al (2006) Central serous chorioretinopathy after solid organ transplantation. Ophthalmology 113:805–813

Ferrara D, Mohler KJ, Waheed N et al (2014) En-face enhanced-depth swept-source optical coherence tomography features of chronic central serous chorioretinopathy. Ophthalmology 121:719–726

Fong AH, Li KK, Wong D (2011) Choroidal evaluation using enhanced depth imaging spectral-domain optical coherence tomography in Vogt-Koyanagi-Harada disease. Retina 31:502–509

Fujimoto H, Gomi F, Wakabayashi T et al (2008) Morphologic changes in acute central serous chorioretinopathy evaluated by Fourier-domain optical coherence tomography. Ophthalmology 115: 1494–1500

Fung AT, Yannuzzi LA, Freund KB (2012) Type 1 (subretinal pigment epithelial) neovascularization in central serous chorioretinopathy masquerading as neovascular age-related macular degeneration. Retina 32:1829–1837

Gäckle HC, Lang GE, Freissler KA et al (1998a) Central serous chorioretinopathy. Clinical, fluorescein angiography and demographic aspects. Ophthalmologe 95:529–533

Gäckle HC, Lang GE, Freidler KA et al (1998b) Clinical fluorescein angiographic and demographic aspects in central serous chorioretinopathy. Ophthalmologe 95:529–533

Gass JDM (1967) Pathogenesis of disciform detachment of the neuroepithelium: II. Idiopathic central serous choroidopathy. Am J Ophthalmol 63:587–615

Gass JDM (1973) Bullous retinal detachment. An unusual manifestation of idiopathic central serous choroidopathy. Am J Ophthalmol 75:810–882

Gass JDM (1991) Central serous chorioretinopathy and white subretinal exudation during pregnancy. Arch Ophthalmol 109:677–681

Gass JDM (1992) Bullous retinal detachment and multiple retinal pigment epithelium detachments in patients receiving haemodialysis. Graefes Arch ClinExpOphthalmol 230:454–458

Gass JDM, Little H (1995) Bilateral bullous exudative retinal detachment complicating idiopathic central serous chorioretinopathy during systemic corticosteroid therapy. Ophthalmology 102:737–747

Gupta V, Gupta A, Gupta P et al (2009) Spectral-domain cirrus optical coherence tomography of choroidal striations seen in the acute stage of Vogt-Koyanagi-Harada disease. Am J Ophthalmol 147:148–153

Gupta V, Gupta P, Dogra MR et al (2010a) Spontaneous closure of retinal pigment epithelium microrip in the natural course of central serous chorioretinopathy. Eye (Lond) 24:595–599

Gupta P, Gupta V, Dogra MR et al (2010b) Morphological changes in the retinal pigment epithelium on spectral-domain OCT in the unaffected eyes with idiopathic central serous chorioretinopathy. Int Ophthalmol 30:175–181

Hooymans JM (1998) Fibrotic scar formation in central serous chorioretinopathy developed during systemic treatment with corticosteroids. Graefes Arch Clin Exp Ophthalmol 236:876–879

Iida T, Spaide RF, Haas A et al (2002) Leopard-spot pattern of yellowish subretinal deposits in central serous chorioretinopathy. Arch Ophthalmol 120:37–42

Imamura Y, Fujiwara T, Margolis R et al (2009) Enhanced depth imaging optical coherence tomography of the choroid in central serous chorioretinopathy. Retina 29:1469–1473

Imamura Y, Fujiwara T, Spaide RF (2011) Fundus autofluorescence and visual acuity in central serous chorioretinopathy. Ophthalmology 118:700–705

Ishihara K, Hangai M, Kita M et al (2009) Acute Vogt-Koyanagi-Harada disease in enhanced spectral-domain optical coherence tomography. Ophthalmology 116:1799–1807

Kim HC, Cho WB, Chung H (2012) Morphologic changes in acute central serous chorioretinopathy using spectral domain optical coherence tomography. Korean J Ophthalmol 26:347–354

Kim SK, Kim SW, Oh J et al (2013) Near-infrared and short-wavelength autofluorescence in resolved central serous chorioretinopathy: association with outer retinal layer abnormalities. Am J Ophthalmol 156:157–164

Kitaya N, Nagaoka T, Hikichi T et al (2003) Features of abnormal choroidal circulation in central serous chorioretinopathy. Br J Ophthalmol 87:709–712

Koizumi H, Yamagishi T, Yamazaki T et al (2013) Relationship between clinical characteristics of polypoidal choroidal vasculopathy and choroidal vascular hyperpermeability. Am J Ophthalmol 155:305–313

Konstantinidis L, Mantel I, Zografos L et al (2010) Intravitreal ranibizumab in the treatment of choroidal neovascularization associated with idiopathic central serous chorioretinopathy. Eur J Ophthalmol 20: 955–958

Lanzetta P, Furlan F, Morgante L et al (2008) Nonvisible subthreshold micropulse diode laser (810 nm) treatment of central serous chorioretinopathy. A pilot study. Eur J Ophthalmol 18:934–940

Lee JH, Lee WK (2014) Choroidal neovascularization associated with focal choroidal excavation. Am J Ophthalmol 157:710–718

Lee SB, Kim JY, Kim WJ et al (2013) Bilateral central serous chorioretinopathy with retinal pigment

epithelium tears following epidural steroid injection. In J Ophthalmol 61:514–515
Lee CS, Woo SJ, Kim YK et al (2014) Clinical and spectral-domain optical coherence tomography findings in patients with focal choroidal excavation. Ophthalmology 121:1029–1035
Lehmann M, Wolff B, Vasseur V et al (2013) Retinal and choroidal changes observed with 'En-face' enhanced-depth imaging OCT in central serous chorioretinopathy. Br J Ophthalmol 97:1181–1186
Levine R, Brucker AJ, Robinson F (1989) Long-term follow-up of idiopathic central serous chorioretinopathy by fluorescein angiography. Ophthalmology 96:854–859
Liegl R, Ulbig MW (2014) Central serous chorioretinopathy. Ophthalmologica 232:65–76, Epub ahead of print
Lumbroso B, Savastano MC, Rispoli M et al (2011) Morphologic differences, according to etiology, in pigment epithelial detachments by means of en-face optical coherence tomography. Retina 31:553–558
Luk FO, Fok AC, Lee A et al (2015) Focal choroidal excavation in patients with central serous chorioretinopathy. Eye (Lond) 29:453–459
Maruko I, Iida T, Sugano Y et al (2010) Subfoveal choroidal thickness after treatment of central serous chorioretinopathy. Ophthalmology 117:1792–1799
Maruko I, Iida T, Ojima A et al (2011a) Subretinal dot-like precipitates and yellow material in central serous chorioretinopathy. Retina 31:759–765
Maruko I, Tomohiro I, Sugano Y et al (2011b) Subfoveal choroidal thickness after treatment of Vogt-Koyanagi-Harada disease. Retina 31:510–517
Matsumoto H, Sato T, Kishi S (2009) Outer nuclear layer thickness at the fovea determines visual outcomes in resolved central serous chorioretinopathy. Am J Ophthalmol 148:105–110
Matsunaga H, Nangoh K, Uyama M et al (1995) Occurrence of choroidal neovascularization following photocoagulation treatment for central serous retinopathy. Nippon GankaGakkaiZasshi 99:460–468
Miki A, Kondo N, Yanagisawa S et al (2014) Common variants in the complement factor h gene confer genetic susceptibility to central serous chorioretinopathy. Ophthalmology 121:1067–1072
Montero JA, Ruiz-Moreno JM, Fernandez-Muñoz M (2011) Intravitreal bevacizumab to treat choroidal neovascularization following photodynamic therapy in central serous choroidopathy. Eur J Ophthalmol 21:503–505
Mrejen S, Spaide RF (2013) Optical coherence tomography: imaging of the choroid and beyond. Surv Ophthalmol 58:387–429
Nair U, Ganekal S, Soman M et al (2012) Correlation of spectral domain optical coherence tomography findings in acute central serous chorioretinopathy with visual acuity. Clin Ophthalmol 6:1949–1954
Nazari H, Hariri A, Hu Z et al (2014) Choroidal atrophy and loss of choriocapillaris in convalescent stage of Vogt-Koyanagi-Harada disease: in vivo documentation. J Ophthalmic Inflamm Infect 4:9
Nicholson B, Noble J, Forooghian F et al (2013) Central serous chorioretinopathy: update on pathophysiology and treatment. Surv Ophthalmol 58:103–126
Nomura Y, Obata R, Yanagi Y (2012) Intravitreal bevacizumab for iatrogenic choroidal neovascularization due to laser photocoagulation in central serous chorioretinopathy. Jpn J Ophthalmol 56:245–249
Odrobina D, Laudańska-Olszewska I, Gozdek P et al (2013) Morphologic changes in the foveal photoreceptor layer before and after laser treatment in acute and chronic central serous chorioretinopathy documented in spectral-domain optical coherence tomography. J Ophthalmol 2013:361513
Ojima Y, Hangai M, Sasahara M et al (2007) Three-dimensional imaging of the foveal photoreceptor layer in central serous chorioretinopathy using high-speed optical coherence tomography. Ophthalmology 114:2197–2207
Ooto S, Tsujikawa A, Mori S et al (2010) Thickness of photoreceptor layers in polypoidal choroidal vasculopathy and central serous chorioretinopathy. Graefes Arch Clin Exp Ophthalmol 248:1077–1086
Ooto S, Tsujikawa A, Mori S et al (2011) Retinal microstructural abnormalities in central serous chorioretinopathy and polypoidal choroidal vasculopathy. Retina 31:527–534
Otsuka S, Ohnba N, Nakao K (2002) A long-term follow-up study of severe variant of central serous chorioretinopathy. Retina 22:25–32
Ozdemir O, Erol MK (2014) Morphologic changes and visual outcomes in resolved central serous chorioretinopathy treated with ranibizumab. Cutan Ocul Toxicol 33(2):122–126, Epub ahead of print
Polak BCP, Baarsma GS, Snyers B (1995) Diffuse retinal pigment epitheliopathy complicating systemic corticosteroid treatment. Br J Ophthalmol 79:922–925
Pryds A, Larsen M (2013) Foveal function and thickness after verteporfin photodynamic therapy in central serous chorioretinopathy with hyperautofluorescent subretinal deposits. Retina 33:128–135
Quin G, Liew G, Ho IV et al (2013) Diagnosis and interventions for central serous chorioretinopathy: review and update. Clin Exp Ophthalmol 41:187–200
Reibaldi M, Cardascia N, Longo A et al (2010) Standard-fluence versus low-fluence photodynamic therapy in chronic central serous chorioretinopathy: a nonrandomized clinical trial. Am J Ophthalmol 149: 307–315
Rogers AH, Martidis A, Greenberg PB et al (2002) Optical coherence tomography findings following photodynamic therapy of choroidal neovascularization. Am J Ophthalmol 134:566–576
Roisman L, Magalhães FP, Lavinsky D et al (2013) Micropulse diode laser treatment for chronic central serous chorioretinopathy: a randomized pilot trial. Ophthalmic Surg Lasers Imaging Retina 44:465–470
Ross A, Ross AH, Mohamed Q (2011) Review and update of central serous chorioretinopathy. Curr Opin Ophthalmol 22:166–173

Sahu DK, Namperumalsamy P, Hilton GF et al (2000) Bullous variant of idiopathic central serous chorioretinopathy. Br J Ophthalmol 84:485–492

Sakata VM, da Silva FT, Hirata CE et al (2014) Choroidal bulging in patients with Vogt-Koyanagi-Harada disease in the non-acute uveitic stage. J Ophthalmic Inflamm Infect 4:6

Sasahara M, Tsujikawa A, Musashi K et al (2006) Polypoidal choroidal vasculopathy with choroidal vascular hyperpermeability. Am J Ophthalmol 142:601–607

Sato T, Kishi S, Watanabe G, Matsumoto H, Mukai R (2007) Tomographic features of branching vascular networks in polypoidal choroidal vasculopathy. Retina 27:589–594

Schatz H, McDonald HR, Johnson RN et al (1995) Subretinal fibrosis in central serous chorioretinopathy. Ophthalmology 102:1077–1088

Sekiryu T, Iida T, Maruko I et al (2010) Infrared fundus autofluorescence and central serous chorioretinopathy. Invest Ophthalmol Vis Sci 51:4956–4962

Shinojima A, Hirose T, Mori R et al (2010) Morphologic findings in acute central serous chorioretinopathy using spectral domain-optical coherence tomography with simultaneous angiography. Retina 30:193–202

Song IS, Shin YU, Lee BR (2012) Time-periodic characteristics in the morphology of idiopathic central serous chorioretinopathy evaluated by volume scan using spectral-domain optical coherence tomography. Am J Ophthalmol 154:366–375

Spaide RF, Koizumi H, Pozzoni MC (2008) Enhanced depth imaging spectral-domain optical coherence tomography. Am J Ophthalmol 146:496–500

Suzuki M, Gomi F, Hara C et al (2014) Characteristics of central serous chorioretinopathy complicated by focal choroidal excavation. Retina 4(6):1216–1222 [Epub ahead of print]

Vasconcelos-Santos DV, Sohn EH, Sadda S et al (2010) Retinal pigment epithelial changes in chronic Vogt-Koyanagi-Harada disease: fundus autofluorescence and spectral domain-optical coherence tomography findings. Retina 30:33–41

Von Graefe A (1866) Ueber central recidivierende retinitis. Graefes Arch Clin Exp Ophthalmol 12:211–215

Wang M, Sander B, la Cour M et al (2005) Clinical characteristics of subretinal deposits in central serous chorioretinopathy. Acta Ophthalmol Scand 83:691–696

Wojtkowski M, Srinivasan V, Fujimoto JG et al (2005) Three-dimensional retinal imaging with high speed ultrahigh resolution optical coherence tomography. Ophthalmology 112:1734–1746

Yalcinbayir O, Gelisken O, Akova-Budak B et al (2014) Correlation of spectral domain optical coherence tomography findings and visual acuity in central serous chorioretinopathy. Retina 34:705–712

Yang L, Jonas JB, Wei W et al (2013) Optical coherence tomography assisted enhanced depth imaging of central serous chorioretinopathy. Invest Ophthalmol Vis Sci 54:4659–4665

Yannuzzi LA, Shakin JL, Fisher YL et al (1984) Peripheral retinal detachments and retinal pigment epithelial atrophic tracts secondary to central serous pigment epitheliopathy. Ophthalmology 91:1554–1572

Yannuzzi LA, Slakter JS, Gross NE et al (2012) Indocyanine green angiography-guided photodynamic therapy for treatment of chronic central serous chorioretinopathy: a pilot study. Retina 32(Suppl 1): 288–298